Electronic Supplementary Material (ESI) for New Journal of Chemistry.
This journal is © The Royal Society of Chemistry and the Centre National de la Recherche Scientifique 2018

Eaton's reagent Assisted Aromatic C-C Coupling of Carbazoles for Optoelectronic Applications

Jie Yuan[1], Lu Jin[1], Runfeng Chen[1*], Xingxing Tang[1], Xiang Xie[1], Yuting Tang[1], Wei Huang[1*]

[1]*Key Laboratory for Organic Electronics and Information Displays & Jiangsu Key Laboratory for Biosensors, Institute of Advanced Materials (IAM), Jiangsu National Synergistic Innovation Center for Advanced Materials (SICAM), Nanjing University of Posts & Telecommunications, 9 Wenyuan Road, Nanjing 210023, China*

**Email: iamrfchen@njupt.edu.cn, wei-huang@njupt.edu.cn*

Contents

Synthesis and characterization

Chemicals and solvents purchased from Aldrich or Acros are of analytical grade and were used without further purification. Unless otherwise noted, reactions were carried out under a dry nitrogen atmosphere using standard Schlenk techniques. ^{1}H and ^{13}C-nuclear magnetic resonance (NMR) spectra were recorded on a Bruker Ultra Shield Plus 400 MHz instrument with $CDCl_3$ as the solvent and tetramethylsilane (TMS) as the internal standard. Liquid chromatograph mass spectrometer (LC/MS) was performed on an Agilent 6230 Accurate-Mass TOF LC/MS using a mixed solvent of 10 vol% water and 90 vol% methanol as the eluent. Elemental analysis was performed on an Elementar Vario MICRO elemental analyzer. X-ray photoelectron spectroscopy (XPS) was performed on a KRATOS Axis Supra. High resolution mass spectra were collected by a LCT Premier XE (Waters) HRMS spectrometry. Steady-state and time-resolved photoluminescence were measured on an Edinburgh FLSP920 fluorescence spectrophotometer. A xenon arc lamp (Xe900) was used as the excitation source for the steady-state photoluminescence and a microsecond flash-lamp (uF900) produces short, typically a few μs optical pulses, was used for phosphorescence spectra measurements at 77 K with a 10 ms delay time after the excitation was turned off.

Single crystal was grown by slow evaporation of combined dichloromethane (DCM) and petroleum ether solutions at room temperature. X-ray crystallography was carried out on a Bruker Smart Apex CCD area detector diffractometer using graphite-monochromated Mo-Kα radiation (λ = 0.71073 Å) at 293 K. Cell parameters were retrieved using SMART software and refined using SAINT on all observed reflections. Structures were solved by direct methods using the program SHELX-97 program package. Non-hydrogen atoms were found using alternating difference Fourier syntheses and least-squared refinement cycles and, during the final cycles, were refined anisotropically. Hydrogen atoms were placed in calculated positions and refined as riding atoms with a uniform value of U_{iso}[1]. The crystal structure was analyzed by Diamond 3.2 software.

Thermogravimetric analysis (TGA) was conducted on a Shimadzu DTG-60H thermogravimetric analysis under a heating rate of 10ºC/min and a nitrogen flow rate of 50 cm^3/min. The differential scanning calorimetry (DSC) analysis was performed on a Shimadzu DSC-60A instrument. Ultraviolet-visible (UV-Vis) spectra were obtained using a SHIMADZU UV-3600 UV-VIS-NIR spectrophotometer. Atomic force microscopy (AFM) height map measurements with topographic image area of 5 × 5 μm^2 were carried out on a Bruker Dimension Icon AFM equipped

with Scanasyst-Air peak force tapping mode AFM tips from Bruker.

Cyclic voltammetry (CV) measurement was performed to estimate the highest occupied molecular orbital (HOMO) and the lowest unoccupied molecular orbital (LUMO) from the onset potential of the electrochemical oxidation and reduction waves, respectively[2]. The CV measurements were carried out at room temperature on a CHI660E system in a typical there-electrode cell with a working electrode (glass carbon), a reference electrode (Ag/Ag^+), referenced against ferrocene/ferrocenium (FOC), and a counter electrode (Pt wire) in an acetonitrile solution of Bu4NPF6 (0.1 M) at a sweeping rate of 100 mV s^{-1}. The thin solid film of the optoelectronic molecule was deposited on the surface of the glass carbon working electrode for CV measurement. HOMO and LUMO energy levels (E_{HOMO} and E_{LUMO}) were estimated based on the reference energy level of ferrocene (4.8 eV below the vacuum) according to the following Equations:

$$E_{HOMO} = -[E_{onset}^{Ox} - E_{(Fc/Fc^+)} + 4.8]\, eV \qquad \text{(S1)}$$

$$E_{LUMO} = E_{HOMO} + {}^{opt}E_g \qquad \text{(S2)}$$

where $E_{(Fc/Fc^+)}$ is the onset oxidative voltage of FOC *vs* Ag/Ag^+ and E_{onset}^{Ox} is the onset potentials of the oxidation, ${}^{opt}E_g$ is the optical bandgap.

Density functional theory (DFT) and time-dependent DFT (TD-DFT) calculations were carried out on Gaussian 09 D.01 package[3]. The ground state (S_0) geometry was fully optimized at B3LYP/6-31G(d) level and the optimized stationary point was further characterized by harmonic vibration frequency analysis to ensure that real local minima had been found. The excitation energies in the *n*-th singlet (S_n) and triplet (T_n) states were computed using the TD-DFT method based on the optimized molecular structure at the ground state (S_0). Contour of electrostatic potential (ESP) were obtained also on the ground state geometry to investigate the charge density distribution. The color code of the map was from the deepest red to the deepest blue, when the potential increases in the order of red < orange < yellow < green < blue.

Blue phosphorescent organic light emitting diodes (PhOLEDs) were fabricated by using Iridium(III) [bis(4,6-difluorophenyl)-pyridinato-N,C2'] picolinate (FIrpic) as the blue phosphorescent dopants emitter. In a general procedure, ITO-coated glass substrates were etched, patterned and washed with detergent, deionized water, acetone and ethanol in turn. After ultraviolet (UV)-ozone treating for 4 min, a 30 nm PEDOT: PSS was spin coated on the ITO substrate and

dried at 120ºC in a vacuum oven for 15 min. The other organic layers were deposited by high-vacuum (≈ 4×10^{-4} Pa) thermal evaporation with a rate of 0.1–0.2 nm s^{-1}. The layer thickness and the deposition rate were monitored *in situ* by an oscillating quartz thickness monitor. The devices without encapsulation were measured immediately after the fabrication under ambient atmosphere at room temperature. Electroluminescent (EL) spectra of the devices were measured by a PR655 spectra scan spectrometer. The luminance-voltage and current–voltage characteristics were recorded using an optical power meter and a Keithley 2602 voltage current source. And the external quantum efficiency (EQE) was calculated by Equation 3[2].

$$EQE = \frac{\pi e \eta_{cd/A} \int \lambda p(\lambda) d\lambda}{hcK_m \int p(\lambda)\Phi(\lambda) d\lambda} \qquad \text{(S3)}$$

where $\eta_{cd/A}$ is the current efficiency (cd/A); h is the Planck constant; c is the speed of light in vacuum; λ is the wavelength (nm); e is the electron charge; $p(\lambda)$ is relative electroluminescent intensity at each wavelength; Φ(λ) is the Commision International de l'Eclairage chromaticity (CIE) standard photopic luminous efficiency function; and K_m is a constant of 683 lm/W.

Eaton's reagent assisted direct C-C cross-coupling for the preparation of 9,9'-diphenyl-9H,9'H-3,3'-bicarbazole (DPhBCz)

Under nitrogen atmosphere, 9-phenyl-9H-carbazole (**PhCz**) (1.50 g, 6.2 mmol) was placed in an oven-dried round-bottom schlenk flask at room temperature. The starting material was heated to be fully melted at 110°C. Then, Eaton's reagent[4] (0.78 mL) was added drop-wise in 5 min and the resulting mixture was stirred at 110°C for 12 hours under the protection of nitrogen. To end the reaction, the mixture was cooled to room temperature, quenched with 3 mL water or saturated aqueous sodium bicarbonate solution for three times. The reaction mixture was diluted with DCM and washed with brine for three times. The organic layers were collected and dried over $MgSO_4$. By removing the organic solvent under reduced pressure, the blackish product was further purified by column chromatography using petroleum ether: DCM (10:1, v/v) as the eluent. Yield: 0.69 g of white powder (46%). ^{1}H NMR (400 MHz, $CDCl_3$): δ= 8.47 (s, 2H), 8.26-8.24 (d, 2H), 7.80-7.77 (d, 2H), 7.67-7.59 (m, 8H), 7.53-7.42 (m, 8H), 7.36-7.26 (m, 2H). ^{13}C NMR (100 MHz, $CDCl_3$): δ= 141.37, 140.05, 137.80, 134.38, 129.93, 127.46, 127.10, 126.06, 125.85, 123.99, 123.58, 120.44, 120.00, 118.91, 110.03, 109.91. MS (ESI) calculated for $C_{18}H_{13}N$: 484.194, found: 483.930. HRMS ($[M + 1]^+$, FAB): calcd. for $C_{36}H_{24}N_2$, 484.1939; found, 484.1931. Anal. calcd. for $C_{36}H_{21}N_2$: C 89.23, H 4.99, N 5.78; found: C 89.02, H 4.94, N 5.66.

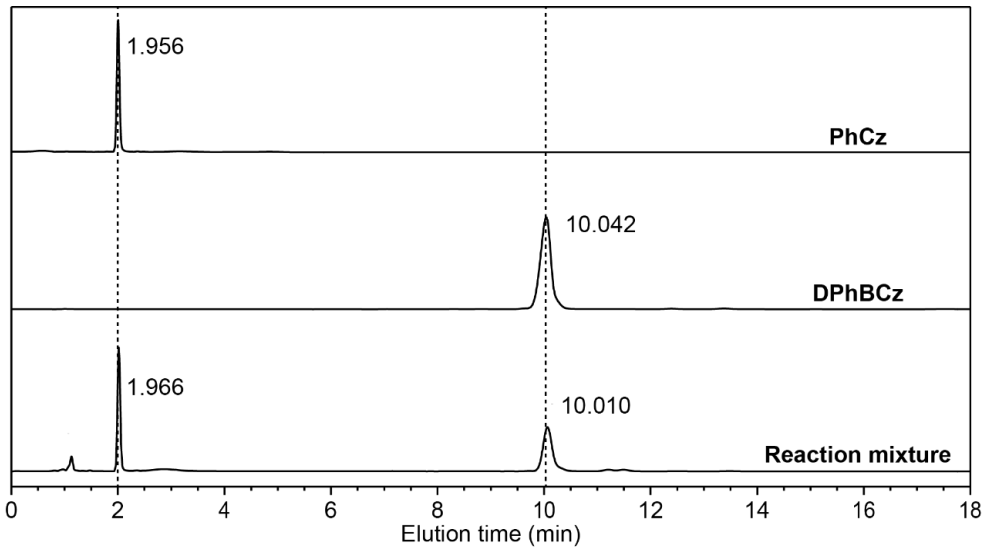

Figure S1. Liquid chromatographs of **PhCz, DPhBCz**, and the reaction mixture after the removal of Eaton's reagent by water washing.

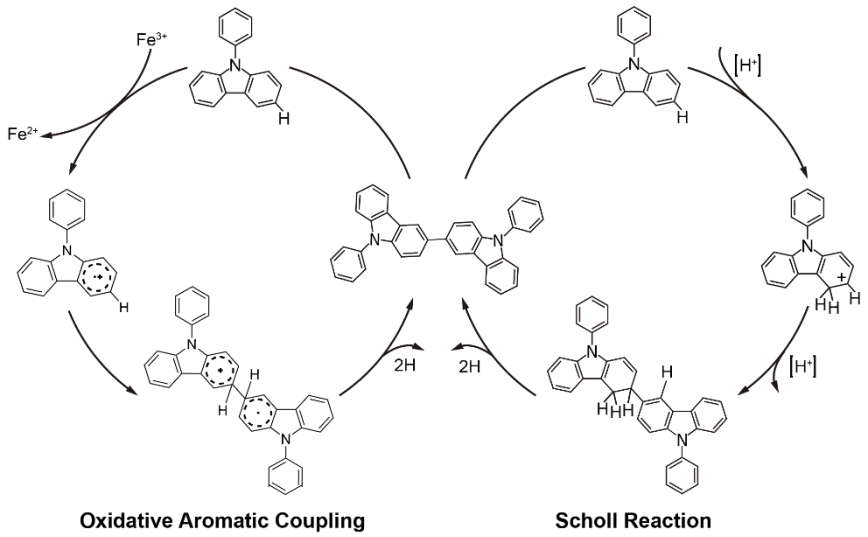

Figure S2. Comparison of oxidative coupling and Scholl reaction for the preparation of **DPhBCz**.

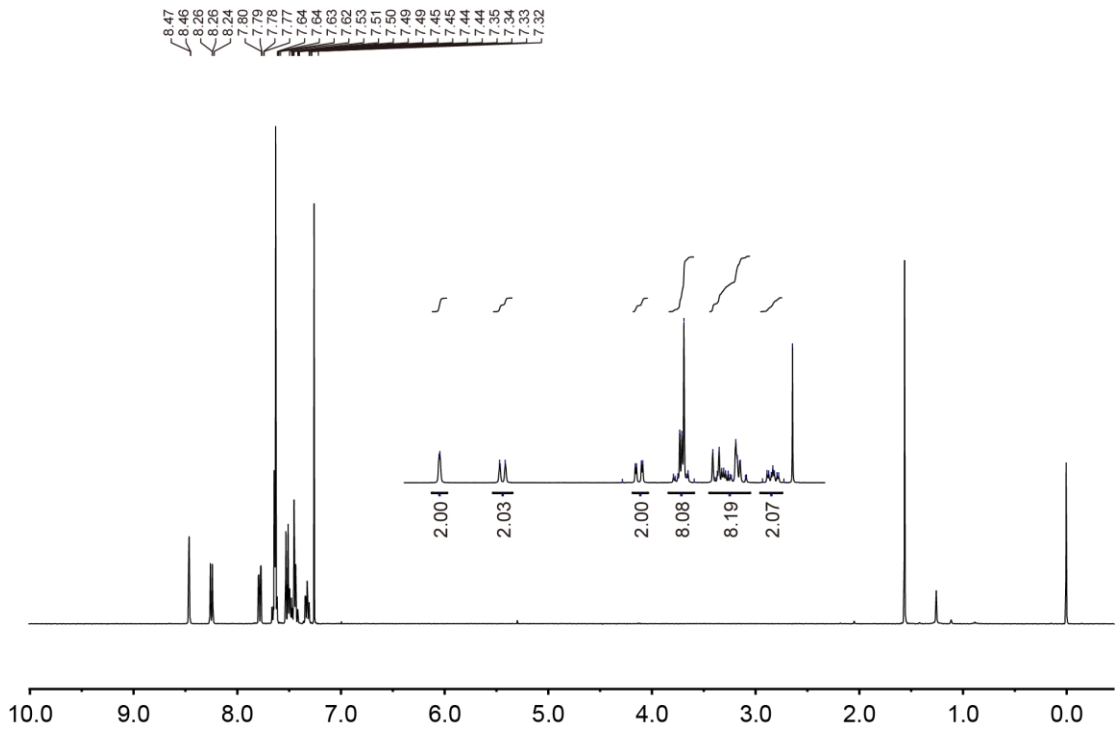

Figure S3. ^{1}H NMR of **DPhBCz** in $CDCl_3$**.**

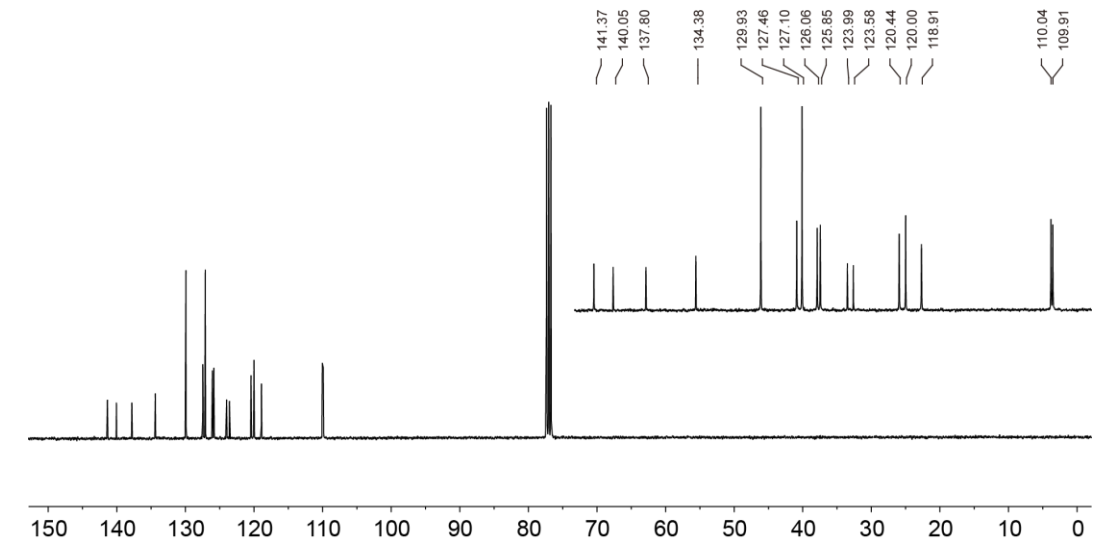

Figure S4. ^{13}C NMR of **DPhBCz** in $CDCl_3$**.**

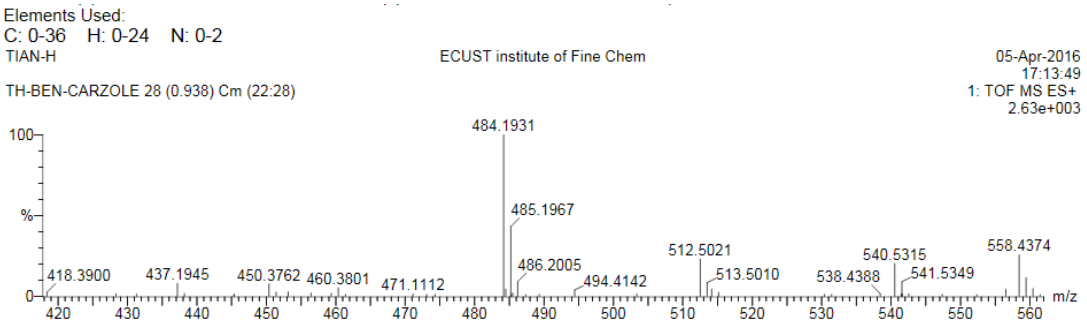

Figure S5. HRMS spectrum of **DPhBCz.**

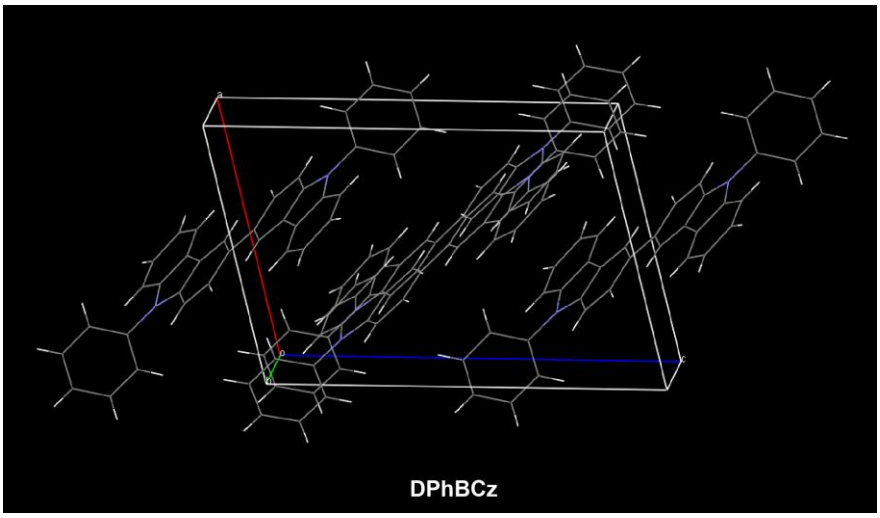

Figure S6. Single-crystal unit cell of **DPhBCz**.

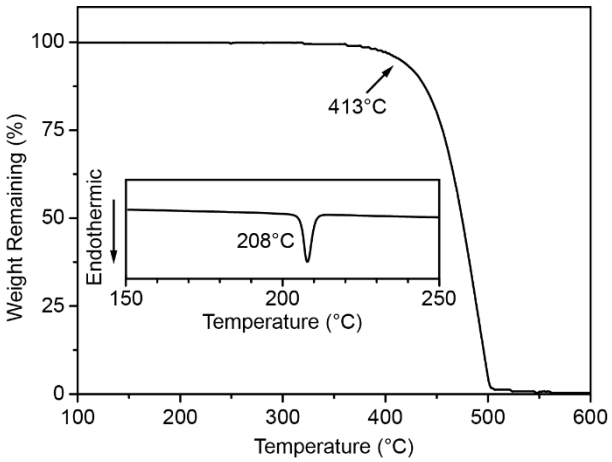

Figure S7. TGA and DSC curves of **DPhBCz.**

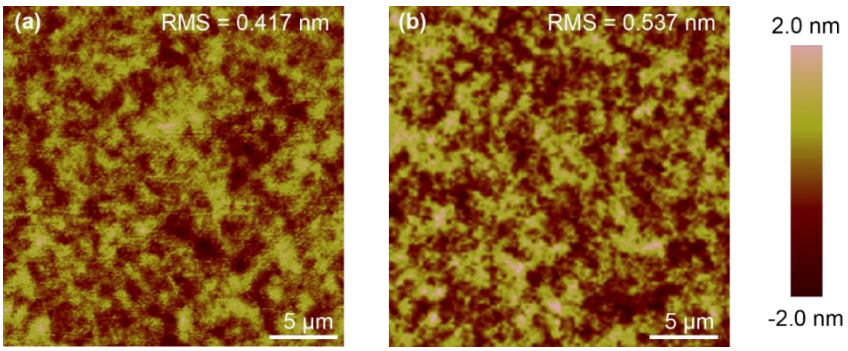

Figure S8. AFM height images of vacuum evaporated (a) pure **DPhBCz** and (b) FIrpic-doped (15 wt %) **DPhBCz** films (20 nm) on the surface of ITO/PEDOT:PSS (30 nm).

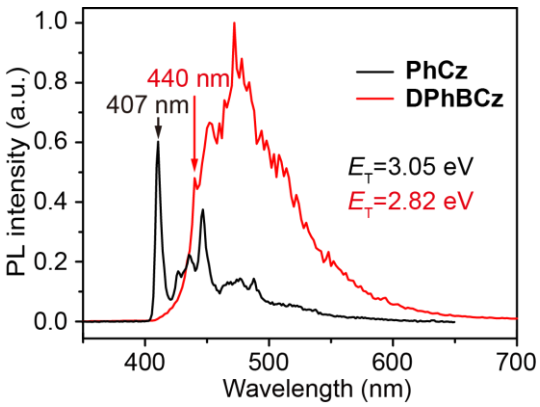

Figure S9. Phosphorescence spectra of **PhCz** and **DPhBCz** in 2-methyltetrahydrofuran excited by 295 nm UV-light at 77 K with a delay time of 10 ms.

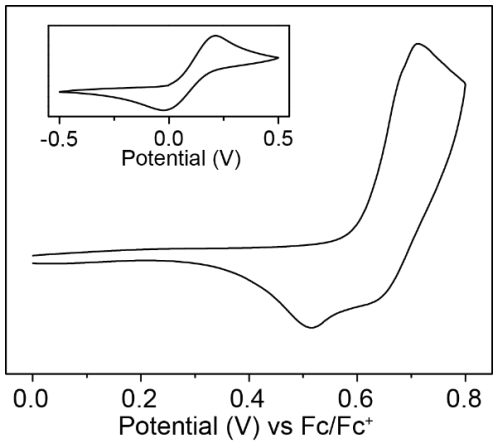

Figure S10. Cyclic voltammogram curve of **DPhBCz** film during the oxidative scan. The insert graph shows the oxidation wave of ferrocene under the identical electrochemical conditions.

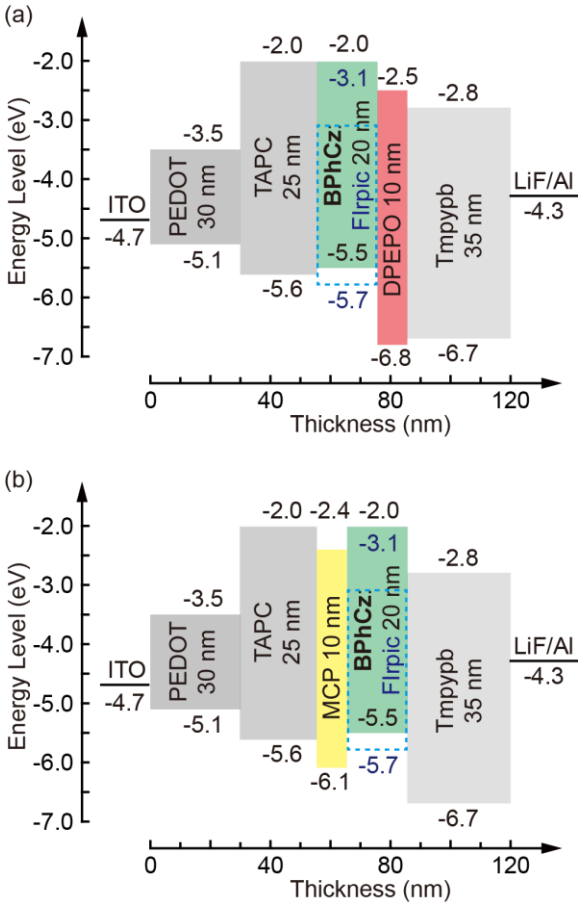

Figure S11. DPhBCz-hosted blue PhOLEDs based on FIrpic in two different device structures of (a) Device A and (b) Device B.

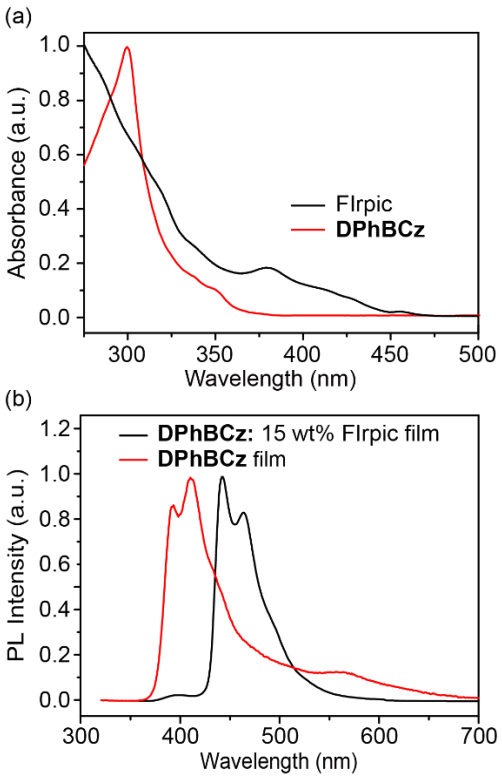

Figure S12. (a) UV-vis absorption spectra of FIrpic and **DPhBCz** in dilute CH_2Cl_2 and (b) PL spectra of **DPhBCz** and **DPhBCz**:15 wt% FIrpic film excited at 295 nm at room temperature. Noted that the **DPhBCz**:15 wt% FIrpic composite film shows typical FIrpic emission bands, demonstrating the efficient energy transfer from the host of **DPhBCz** to the guest of FIrpic.

Table S1. A brief comparison of various methods in preparing bicarbazoles.

Starting material	Target product	Reaction condition	Yield	Ref.
9H-carbazole **(Cz)**	9H,9'H-3,3'-bicarbazole **(BCz)**	Oxidative coupling: $FeCl_3$, $CHCl_3$, N_2, rt, 0.5 h	62%	[5]
3-Bromo-9H-carbazole **(BrCz)**	9H,9'H-3,3'-bicarbazole **(BCz)**	(1) Boronation: $Pd(dppf)Cl_2$, KOAc, dioxane, 80°C, 24 h. (2) Suzuki coupling: $Pd[P(C_6H_5)_3]_4$, PhMe, K_2CO_3, N_2, 110°C, 24 h.	48%[a]	[6,7]
9H,9'H-3,3'-bicarbazole (**BCz**)	9,9'-Diphenyl-9H,9'H-3,3'-bicarbazole **(DPhBCz)**	Ullmann reaction: CuI, PhBr, K_2CO_3, DMF	67%	[8]
9-Phenyl-carbazole **(PhCz)**	9,9'-Diphenyl-9H,9'H-3,3'-bicarbazole **(DPhBCz)**	Oxidative coupling: $FeCl_3$, $CHCl_3$, N_2, rt, 1 h.	35%	[9]
9H-carbazole **(Cz)**	9,9'-Diphenyl-9H,9'H-3,3'-bicarbazole **(DPhBCz)**	(1) Ullmann reaction: CuI, PhI, K_2CO_3, DMF, 165°C, 24 h. Yield: 95% (2) C-C coupling: Eaton's reagent, N_2, 110°C, 12 h.	44%	This work
9-Phenyl-carbazole **(PhCz)**	9,9'-Diphenyl-9H,9'H-3,3'-bicarbazole **(DPhBCz)**	Eaton's reagent, N_2, 110°C, 12 h.	46%	This work

[a] The total yield was calculated from that of two steps using 81%×59%=48%.

Table S2. Optimization of reaction conditions.[a]

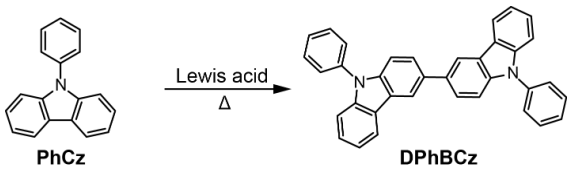

Entry	Lewis acid	Usage	Equiv. of P_2O_5	Solvent	Atmosphere	Temp. (°C)	Time (h)	Yield (%)
1	Eaton's reagent	0.40 mL	0.05	None	N_2	110	12	21
2	Eaton's reagent	0.78 mL	0.1	None	N_2	110	12	46
3	Eaton's reagent	1.56 mL	0.2	None	N_2	110	12	35
4	Eaton's reagent	0.78 mL	0.1	None	N_2	110	6	30
5	Eaton's reagent	0.78 mL	0.1	None	N_2	110	18	40
6	Eaton's reagent	0.78 mL	0.1	None	N_2	90	12	0
7	Eaton's reagent	0.78 mL	0.1	None	N_2	100	12	13
8	Eaton's reagent	0.78 mL	0.1	None	N_2	120	12	45
9	Eaton's reagent	0.78 mL	0.1	None	N_2	130	12	6
10	P_2O_5	0.09 g	0.1	None	N_2	110	12	0
11	Methanesulfonic acid	0.73 mL	0.1	None	N_2	110	12	0
12	Eaton's reagent	0.78 mL	0.1	DCM	N_2	110	12	0
13	Eaton's reagent	0.78 mL	0.1	None	Air	110	12	14

[a] In all the reactions, 1.50 g **PhCz** (6.2 mmol) was used and the Eaton's reagent contains 7.5 wt% P_2O_5 in methanesulfonic acid.

Table S3. Crystallographic data of **DPhBCz** single crystal.

Compound	**DPhBCz**
Empirical formula	$C_{36}H_{24}N_2$
Formula weight (g mol^{-1})	484.57
Crystal color	colorless
Wavelength (Å)	0.71073
Space Group	P 21/c
a (Å)	9.4067(11)
b (Å)	9.6150(11)
c (Å)	14.1821(16)
α (deg)	90
β (deg)	104.252(3)
γ (deg)	90
V (Å^3)	1243.2(2)
Z	2
Density (g cm^{-3})	1.294
μ (mm^{-1})	0.075
T_{min}, T_{max}	0.991, 0.993
F(000)	508.0
h_{max}, k_{max}, l_{max}	12, 12, 18
$Theta_{max}$	28.220
Goof	1.093
Refinement parameters	R_1 =0.0502 (2567) wR_2=0.1213 (3002)

Table S4. Thermal, photophysical, and electrochemical properties of **PhCz** and **DPhBCz** [a].

Compd.	T_m/T_d (°C)	$^s\lambda_{Abs}$ (nm)	$^f\lambda_{abs}$ (nm)	$^s\lambda_{PL}$ (nm)	$^f\lambda_{PL}$ (nm)	$^{opt}E_g$ (eV)	**HOMO/LUMO** (eV)	E_T (eV)
PhCz	97/199	293/327/341	296/332/350	349/364	368	3.60	-5.64/-2.04	3.05
DPhBCz	208/413	304/340/352	308/344/355	389/405	391/410	3.44	-5.45/-2.01	2.82

[a]Absorption (Abs) peaks measured in CH_2Cl_2 solution ($^s\lambda_{abs}$) and thin film ($^f\lambda_{abs}$) as well as photoluminescent (PL) peaks observed in CH_2Cl_2 solution ($^s\lambda_{PL}$) and thin film ($^f\lambda_{PL}$) at the room temperature.Optical energy gap ($^{opt}E_g$) was obtained from the onset of UV-vis spectrum in solid film. HOMO and LUMO energy levels was deduced from Equations S1 and S2. Triplet energy (E_T) was determined by the highest energy vibronic sub-band of the phosphorescence spectrum at 77 K.

Table S5. A brief summary of the recently reported high-performance FIrpic-based PhOLEDs on current efficiency (CE, in $cd \cdot A^{-1}$), external quantum efficiency (EQE, in %), and efficiency roll-off at the brightness of 1000 $cd \cdot m^{-2}$ (in %).

	Maximum efficiency		At 1000 $cd \cdot m^{-2}$		Roll-off (%)	
	CE	EQE	CE	EQE	CE	EQE
Ref. [2]	32.3	16.5	23.4	12.2	27.6	26.1
Ref. [10]	49.6	28.2	38.9	22.1	21.6	21.6
Ref. [7]	53.6	30.1	-	28.4	-	5.6
Ref. [11]	-	31.4	-	28.6	-	8.9
Ref. [12]	58.8	25.3	54.1	23.1	8.0	8.7
Ref. [13]	49.1	23.1	-	20.2	-	12.6
Ref. [14]	-	23.0	-	20.0	-	13.0
Ref. [15]	-	34.1	-	32.2	-	5.6
Ref. [16]	46.4	24.6	42.9	22.8	7.5	7.3
Ref. [17]	52.0	25.1	51.0	24.6	1.9	2.0
Ref. [18]	38.2	19.0	37.3	18.5	2.4	2.6
Ref. [19]	44.7	22.3	42.6	20.1	4.7	9.9
Ref. [20]	39.7	21.7	28.1	15.3	29.2	29.5
Ref. [21]	29.9	16.5	28.6	15.8	4.3	4.2
This work	31.7	16.9	30.0	16.7	5.4	1.2

References

1. Z. H. Sun, J. H. Luo, S. Q. Zhang, C. M. Ji, L. Zhou, S. H. Li, *Adv. Mater.* 2013, **25**, 4159.
2. Y. Tao, J. J. Xiao, C. Zheng, Z. Zhang, M. K. Yan, R. F. Chen, X. H. Zhou, H. H. Li, Z. F. An, Z. X. Wang, H. Xu, W. Huang, *Angew. Chem. Int. Ed.* 2013, **52**, 10491.
3. M.J. Frisch, G.W. Trucks, H.B. Schlegel, *Gaussian 09 Gaussian*. Inc.: Wallingford, CT, 2009.
4. P. E. Eaton, G. R. Carlson and J. T. Lee, *J. Org. Chem.*, 1973, **38**, 4071.
5. V. Vaitkeviciene, S. Grigalevicius, J. V. Grazulevicius, V. Jankauskas and V. G. Syromyatnikov, *Eur. Polym. J.*, 2006, **42**, 2254.
6. M. Kim, S. K. Jeon, S. H. Hwang, S. S. Lee, E. Yu and J. Y. Lee, *J. Phys. Chem. C*, 2016, **120**, 2485.
7. M. Kim and J. Y. Lee, *ACS Appl. Mater. Inter.*, 2014, **6**, 14874.
8. H. Sasabe, N.Toyota, H. Nakanishi, T. Ishizaka, Y. J. Pu, and J. Kido, *Adv. Mater.*, 2012, **24**, 3212.
9. G. M. Tang, R. H. Chi, W. Z. Wan, Z. Q. Chen, T. X. Yan, Y. P. Dong, Y. T. Wang and Y. Z. Cui, *J. Lumin.*, 2017, **185**, 1.
10. L. C. Won and L. J. Yeob, *Adv. Mater.*, 2013, **25**, 5450.
11. K. Mounggon and L. J. Yeob, *Adv. Funct. Mater.*, 2014, **24**, 4164.
12. L. Ding, S. C. Dong, Z. Q. Jiang, H. Chen, L. S. Liao, *Adv. Funct. Mater.* 2015, **25**, 645.
13. C. H. Shih, P. Rajamalli, C. A. Wu, M. J. Chiu, L. K. Chu and C. H. Cheng, *J. Mater. Chem. C*, 2015, **3**, 1491.
14. C. W. Lee and J. Y. Lee, *Adv. Mater.*, 2013, **25**, 596.
15. H. Shin,; J. H. Lee,; C. K. Moon,; J. S. Huh,; B. Sim,; J. J. Kim, *Adv. Mater.*, 2016, **28**, 4920.
16. Z. X. Wang, H. D. Wang, J. Zhu, P. Wu, B. Shen, D. H. Dou, B. Wei, *ACS Appl. Mater. & Inter.*, 2017, **9**, 21346.
17. M. M. Xue, C. C. Huang, Y. Yuan, L. S. Cui, Y. X. Li, B. Wang, Z. Q. Jiang, M. K. Fung and L. S. Liao, *ACS Appl. Mater. & Inter.*, 2016, **8**, 20230.
18. C. L. Bian, Q. Wang, X. Y. Liu, J. Fan and L. S. Liao, *Org. Electro.*, 2017, **46**, 105.
19. Z. Zhang, J. W. Xie, Z. X. Wang, B. W. Shen, H. D. Wang, M. J. Li, J. H. Zhang and J. Cao, *J. Mater. Chem. C*, 2016, **4**, 4226.
20. Y. Tao, L. J. Xu, Z. Zhang, R. F. Chen, H. H. Li, H. Xu, C. Zheng and W. Huang, *J. Am. Chem. Soc.*, 2016, **138**, 9655.
21. Y. Tao, X. Guo, L. Hao, R. F. Chen, H. H. Li, Y. H. Chen, X. W. Zhang, W. Y. Lai, W. Huang, *Adv. Mater.*, 2015, **27**, 6939.